ANALYSIS OF THE MULTIMODULUS BLIND EQUALIZATION ALGORITHM FOR NON-SQUARE RECTANGULAR QAM SIGNAL CONSTELLATIONS

Jenq-Tay Yuan and Kun-Da Tsai

Department of Electronic Engineering, Fu Jen Catholic University Taipei 24205, Taiwan, China

E-mail: yuan@ee.fju.edu.tw

Abstract

This work mathematically analyzes a multimodulus blind equalization algorithm (MMA) for non-square rectangular quadrature amplitude modulation (QAM) signal constellations. The analysis indicates that the MMA that uses non-square rectangular constellations may be better able to recover the phase rotation introduced by channels than the MMA that uses either the square or the cross constellations, although the former is known to require more average transmitted power than the latter two. The analysis also demonstrates that the MMA that uses non-square rectangular constellations may be less attracted to saddle points (thus increasing convergence speed) than the MMA that uses cross constellations, because the former has fewer saddle points than the latter.

Index Terms – Blind equalization, constant modulus algorithm (CMA), cross constellations, inter-symbol interference (ISI), multimodulus algorithm (MMA), non-square rectangular constellations, phase-locked loop, quadrature amplitude modulation (QAM), non-square rectangular constellations.

1. Introduction

The analysis in [1] indicate that the multimodulus blind equalization algorithm (MMA) presented therein can remove inter-symbol interference (ISI) and simultaneously correct the phase error because it implicitly incorporates a phase-tracking loop, which automatically recovers the carrier phase. However, [1] addresses only the MMA that uses square constellations. In a companion paper [2], we analyze the MMA for non-square (or cross) QAM signal constellations. However, the N-points constellations ($N = 2^{2i-1}, i \in$ *Integer and* $i \geq 0$) can also be arranged into what we call "*non-square rectangular* constellations", for which $N = 2^x \cdot 2^y = 2^{2i+1}$, where both x and y are positive integers, (for example, in Fig. 1, $32 = 8 \cdot 4 = 16 \cdot 2$.) The MMA that uses cross constellation is more efficient in terms of required average transmitted power, since it requires around 30% less average transmitted power than the MMA that uses the non-square rectangular constellation, for a given probability of error. However, the analysis in this paper reveals that using non-square rectangular constellations provides advantages in blind equalization. These advantages do not appear to exist when both cross signal constellations and square signal constellations are used. Notably, in this paper we will use exactly the same notations as those used throughout the companion paper in [2].

2. MMA Cost Functions

A. General Formulation of MMA Cost Function

The final expansion of the MMA cost function for a complex iid zero-mean source and a complex baseband channel is provided by excluding additive channel noise. Given the assumption that each member of the symbol alphabet is equiprobable in the source sequence, the general formulation of the MMA cost function for both square and non-square constellations (ignoring additive channel noise) can be expressed as

$$\begin{aligned} J_{MMA} = {} & \tfrac{1}{4}\mathrm{Re}\left\{E\{s^4(n)\}\sum h^4(i) + 3E\{s^2(n)\}^2\sum\sum_{i\neq j} h^2(i)h^2(j)\right. \\ & + \tfrac{3}{4}\left(k_s\sigma_s^4\sum_i |h(i)|^4 + 2\sigma_s^4\sum\sum_{i\neq j}|h(i)|^2|h(j)|^2 + \left|E\{s^2(n)\}\right|^2\sum\sum_{i\neq j} h^2(i)(h^*(j))^2\right. \\ & - 2R_{1,R}\left(\tfrac{1}{2}\mathrm{Re}\left\{E\{s^2(n)\}\sum h^2(i)\right\} + \tfrac{1}{2}\left(\sigma_s^2\sum|h(i)|^2\right)\right) \\ & - 2R_{1,I}\left(-\tfrac{1}{2}\mathrm{Re}\left\{E\{s^2(n)\}\sum h^2(i)\right\} + \tfrac{1}{2}\left(\sigma_s^2\sum|h(i)|^2\right)\right) \\ & \left. + R_{1,R}^2 + R_{1,I}^2 \right. \end{aligned} \tag{1}$$

where $\sigma_s^2 = E\left\{|s(n)|^2\right\}$ and $k_s = \dfrac{E\left\{|s(n)|^4\right\}}{\sigma_s^4}$. Notably, the existence of the first term on the right-hand side of (1), $\tfrac{1}{4}\cdot\mathrm{Re}\left[E\{s^4(n)\}\sum h^4(i)\right]$, which contains the phase information of

0-7803-8406-7/04/$20.00 © 2004 IEEE.

the blind equalizer output, reveals that the MMA cost function in equation (1) of [2] employs both the *modulus* and the *phase* of the equalizer output. This phase information allows the MMA, using either the square or the non-square constellation, to recover a possible phase rotation of the equalizer output, resulting from a time-varying phase shift introduced by the channels owing to a discrete-time first-order phase-locked loop hidden inside the MMA. (See also [1].)

B. Cost Function of Non-Square Rectangular Constellations

Equation (1) can be expressed in terms of the real and imaginary parts of *s(n)*:

$$\begin{aligned}
J_{MMA}(n) = {} & \tfrac{1}{4}\left(E\{s_R^4(n)\} + E\{s_I^4(n)\} - 6E\{s_R^2(n)\}E\{s_I^2(n)\}\right)\mathrm{Re}\left\{\sum_i h^4(i)\right\} \\
& + 3\left(E^2\{s_R^2(n)\} + E^2\{s_I^2(n)\} - 2\cdot E\{s_R^2(n)\}E\{s_I^2(n)\}\right)\mathrm{Re}\left\{\sum_i\sum_{i\neq j} h^2(i)\cdot h^2(j)\right\} \\
& + \tfrac{3}{4}\left(E\{s_R^4(n)\} + E\{s_I^4(n)\} + 2\cdot E\{s_R^2(n)\}E\{s_I^2(n)\}\right)\sum_i |h(i)|^4 \\
& + 2\left(E^2\{s_R^2(n)\} + E^2\{s_I^2(n)\} + 2E\{s_R^2(n)\}E\{s_I^2(n)\}\right)\sum_i\sum_{i\neq j} |h(i)|^2|h(j)|^2 \\
& - \left(E^2\{s_R^2(n)\} + E^2\{s_I^2(n)\} - 2E\{s_R^2(n)\}E\{s_I^2(n)\}\right)\sum_i\sum_{i\neq j} h^2(i)|h^2(j)| \\
& - 2R_{2,R}\left(\tfrac{1}{2}\left(E\{s_R^4(n)\} - E\{s_I^4(n)\}\right)\mathrm{Re}\left\{\sum_i h^2(i)\right\} + \tfrac{1}{2}\left(E\{s_R^2(n)\} + E\{s_I^2(n)\}\right)\sum_i |h(i)|^2\right) \\
& - 2R_{2,I}\left(-\tfrac{1}{2}\left(E\{s_R^4(n)\} - E\{s_I^4(n)\}\right)\mathrm{Re}\left\{\sum_i h^2(i)\right\} + \tfrac{1}{2}\left(E\{s_R^2(n)\} + E\{s_I^2(n)\}\right)\sum_i |h(i)|^2\right) \\
& + R_{2,R}^2 + R_{2,I}^2 \qquad (2)
\end{aligned}$$

where $s_R(n)$ and $s_I(n)$, are independent of each other and both are zero-mean, sub-Gaussian. However, unlike for square constellations, for non-square rectangular constellations, $R_{2,R} \neq R_{2,I}$ and $E\{s_R^4(n)\} \neq E\{s_I^4(n)\}$, and $E\{s_R^2(n)\} \neq E\{s_I^2(n)\}$.

Consequently, a variable $\rho = \dfrac{E\{s_I^2(n)\}}{E\{s_R^2(n)\}}$ is defined to relate the statistics of the real part of the source symbols to those of the imaginary part of the source symbols.

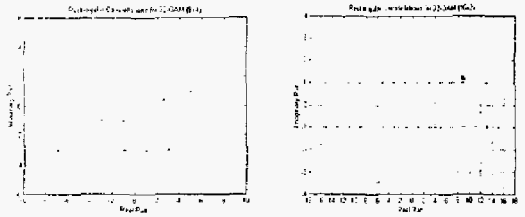

Fig. 1 Two possible non-square rectangular constellations for 32-QAM

3. Analysis of MMA Using Non-Square Rectangular Constellations

A. Unstable Equilibria of the MMA when $M \geq 2$

If the distribution of *s(n)* is sub-Gaussian (such that $\left(E\{s_R^4(n)\} - 3E^2\{s_R^2(n)\}\right) < 0$), then all the pre-specified $\mathbf{h}_M$ (with the associated I_M), for $M \geq 2$, can be shown to be unstable equilibria (saddle points) by applying the concept proposed by Foschini [3], (i.e., *(a)* decrease the cost function of the MMA by a perturbation of two nonzero components of $\mathbf{h}_M$ that leaves $\sum_k |h_M(k)|^2$ invariant, and (b) increase the cost function of the MMA by a perturbation that increases the magnitude of a zero component by a sufficiently small positive number). Consequently, $\mathbf{h}_M$ can only be a saddle point such that all the stationary points are saddle points when $M \geq 2$.

B. Stationary Points of MMA when $M = 1$

When $M=1$ (as in steady-state mode), the combined channel-equalizer impulse response vector $\mathbf{h}_M = [\ldots, h_M(-1), h_M(0), h_M(1), \ldots]^T = \mathbf{h}_1 = [0,0,\ldots,0,h(k),0,\ldots,0,0]^T$, where $h(k) = h_R(k) + jh_I(k)$. Using $\begin{cases} r(k) = \sqrt{h_R^2(k) + h_I^2(k)}, \\ \theta(k) = \tan^{-1}\dfrac{h_I(k)}{h_R(k)}, \end{cases}$ (2) can be reduced to

$$\begin{aligned}
J_{MMA}(n) = {} & \tfrac{1}{4}\left(E\{s_R^4(n)\} + E\{s_I^4(n)\} - 6E\{s_R^2(n)\}E\{s_I^2(n)\}\right)\sum_i r^4(i)\cos 4\cdot\theta(i) \\
& + \tfrac{3}{4}\left(\left(E\{s_R^4(n)\} + E\{s_I^4(n)\} + 2E\{s_R^2(n)\}E\{s_I^2(n)\}\right)\sum_i r^4(i)\right) \\
& - \left(E\{s_R^4(n)\}(1-\rho)\sum_i r^2(i)\cos 2\theta(i) + E\{s_R^4(n)\}(1+\rho)\sum_i r^2(i)\right) \\
& - \left(E\{s_I^4(n)\}\left(1-\tfrac{1}{\rho}\right)\sum_i r^2(i)\cos 2\theta(i) + E\{s_I^4(n)\}\left(1+\tfrac{1}{\rho}\right)\sum_i r^2(i)\right) \\
& + R_{2,R}^2 + R_{2,I}^2 \qquad (3)
\end{aligned}$$

Notably, the MMA cost function for square constellations with $M = 1$ is merely a special case of (3) when ρ is set to be unity.

The set of stationary points of the MMA for non-square rectangular constellations given $M = 1$ can be obtained by setting the gradient of $J_{MMA}(n)$ in (3) to zero, such that $\nabla J_{MMA}(n) = \mathbf{r}\dfrac{\partial J_{MMA}(n)}{\partial r(k)} + \dfrac{\boldsymbol{\theta}}{r(k)}\dfrac{\partial J_{MMA}(n)}{\partial\theta(k)} = 0$ yields

$$\frac{\partial J_{MMA}}{\partial r(k)} = 0 = \left(E\{s_R^4(n)\} + E\{s_I^4(n)\} - 6E\{s_R^2(n)\}E\{s_I^2(n)\}\right)r^3(k)\cos 4\cdot\theta(k) + 3\left(E\{s_R^4(n)\} + E\{s_I^4(n)\} + 2E\{s_R^2(n)\}E\{s_I^2(n)\}\right)r^3(k) - \left(E\{s_R^2(n)\}(1-\rho)2r(k)\cos 2\theta(k) + E\{s_R^4(n)\}(1+\rho)2r(k)\right) - \left(E\{s_I^4(n)\}\left(1-\frac{1}{\rho}\right)2r(k)\cos 2\cdot\theta(k) + E\{s_I^4(n)\}\left(1+\frac{1}{\rho}\right)2r(k)\right) \quad (4)$$

$$\frac{1}{r(k)}\frac{\partial J_{MMA}}{\partial\theta(k)} = 0 = \left(E\{s_R^4(n)\} + E\{s_I^4(n)\} - 6E\{s_R^2(n)\}E\{s_I^2(n)\}\right)r^3(k)\sin 4\theta(k) - \left(E\{s_R^2(n)\}(1-\rho)2r(k)\sin 2\cdot\theta(k)\right) - \left(E\{s_I^2(n)\}\left(1-\frac{1}{\rho}\right)2r(k)\sin 2\theta(k)\right) \quad (5)$$

Solving (4) and (5) simultaneously yields the following possible stationary points:

$$r(k) = 0 \quad (6a)$$

$$r(k) = 1 \qquad \theta(k) = 0 \text{ or } \pi \quad (6b)$$

$$r^2(k) = \frac{\rho E\{s_R^4(n)\} + \frac{1}{\rho}E\{s_I^4(n)\}}{E\{s_R^4(n)\} + E\{s_I^4(n)\}}, \qquad \theta(k) = \pi/2 \text{ or } 3\pi/2 \quad (6c)$$

$$r^2(k) = \frac{(1-\rho)E\{s_R^4(n)\} + \left(1+\frac{1}{\rho}\right)E\{s_I^4(n)\}}{E\{s_R^4(n)\} + E\{s_I^4(n)\} + 6E\{s_R^2(n)\}E\{s_I^2(n)\}}, \quad \theta(k) = \frac{1}{2}\cos^{-1}\left(\frac{(1-\rho)E\{s_R^4(n)\} + \left(1-\frac{1}{\rho}\right)E\{s_I^4(n)\}}{\left(E\{s_R^4(n)\} + E\{s_I^4(n)\} - 6E\{s_R^2(n)\}E\{s_I^2(n)\}\right)r^2(k)}\right) \quad (6d)$$

Note that the locations of the stationary points described by (6a) and (6b) are unaffected by the value of ρ, where ρ determines the type of non-square rectangular constellations, as indicated in Table I. This finding reveals that the locations of these three stationary points ($[h_R(k), h_I(k)] = [0,0]$ and $[h_R(k), h_I(k)] = [\pm 1, 0]$) are fixed and that they always exist for both square and non-square rectangular constellations. However, stationary points specified in (6d) do not exist for all types of non-square rectangular constellations because

$$-1 \le \frac{(1-\rho)E\{s_R^4(n)\} + \left(1-\frac{1}{\rho}\right)E\{s_I^4(n)\}}{\left(E\{s_R^4(n)\} + E\{s_I^4(n)\} - 6E\{s_R^2(n)\}E\{s_I^2(n)\}\right)r^2(k)} \le 1$$ is violated for all $\rho \neq 1$. Therefore, the stationary points described by (6d) will not be taken into account herein and only the stationary points described by (6a) – (6c) are considered. Notably, the stationary points specified by (6d) correspond to the four saddle points of the MMA that uses square constellations when $\theta(k) \in \left\{\frac{\pi}{4}, \frac{3\pi}{4}, \frac{5\pi}{4}, \frac{7\pi}{4}\right\}$. Consequently, the four saddle points that exist in square constellations are absent when non-square rectangular constellations are used. This result implies that the MMA that uses non-square rectangular constellations may be less likely to be attracted to the saddle points (possibly increasing convergence speed) than the MMA using cross constellations.

C. Desired Global Minima of MMA and Unstable equilibria of MMA when M = 1

Equation (3) can be used to show straightforwardly that

$$\begin{cases} \frac{\partial^2 J_{MMA}}{\partial h_R^2(k)} = 4\left\{3\left(E\{s_R^4(n)\} + E\{s_I^4(n)\}\right)h_R^2(k) + 6E\{s_R^2(n)\}E\{s_I^2(n)\}h_I^2(k) - R_{2,R}E\{s_R^2(n)\} - R_{2,I}E\{s_I^2(n)\}\right\} \\ \frac{\partial^2 J_{MMA}}{\partial h_I^2(k)} = 4\left\{3\left(E\{s_R^4(n)\} + E\{s_I^4(n)\}\right)h_I^2(k) + 6E\{s_R^2(n)\}E\{s_I^2(n)\}h_R^2(k) - R_{2,R}E\{s_R^2(n)\} - R_{2,I}E\{s_I^2(n)\}\right\} \\ \frac{\partial^2 J_{MMA}}{\partial h_R(k)\partial h_I(k)} = 48\cdot E\{s_R^2(n)\}E\{s_I^2(n)\}h_R(k)h_I(k) \end{cases} \quad (7)$$

The second derivative test on pp. 768 of [5] easily confirms that, for a sub-Gaussian input,

$$\begin{cases} D(0,0) = 16\left(R_{2,R}E\{s_R^4(n)\} + R_{2,I}E\{s_I^2(n)\}\right)\left(R_{2,R}E\{s_I^2(n)\} + R_{2,I}E\{s_R^2(n)\}\right) > 0 \\ \left[\frac{\partial^2 J_{MMA}}{\partial h_R^2(k)}\right]_{h_R(n)=h_I(n)=[0,0]} = -4\left(R_{2,R}E\{s_R^4(n)\} + R_{2,I}E\{s_I^2(n)\}\right) < 0 \end{cases} \quad (8)$$

Accordingly, $[h_R(k), h_I(k)] = [0,0]$ is a local maximum. Similarly, for $r^2(k) = 1$ with $\theta(k) = 0$ *or* $\theta(k) = \pi$, which corresponds to $[h_{1,R}(k), h_{1,I}(k)] = [\pm 1, 0]$, for a sub-Gaussian input,

$$\begin{cases} D[h_R(k), h_I(k)] = 32\left\{E\{s_R^4(n)\}\left(3E\{s_R^2(n)\} - R_{2,R}\right) + E\{s_R^2(n)\}\left(3E\{s_I^2(n)\} - R_{2,I}\right)\right\} > 0 \\ \left[\frac{\partial^2 J_{MMA}}{\partial h_R^2(k)}\right]_{[h_R(n), h_I(n)] = [\pm 1, 0]} = 8\left\{E\{s_R^4(n)\} + E\{s_I^4(n)\}\right\} > 0 \end{cases} \quad (9)$$

Hence $[h_{1,R}(k), h_{1,I}(k)] = [\pm 1, 0]$ are local minima. Notably, equalizer output has a 90^0 phase ambiguity when the quadrantally symmetric QAM square constellations and QAM cross constellations are used because phase errors that are multiples of 90^0 are undetectable. However, for non-square rectangular constellations which are 180^0 symmetric, phase errors that are multiples of 180^0 are undetectable.

Finally, for $r^2(k) = \frac{\rho E\{s_R^4(n)\} + \frac{1}{\rho}E\{s_I^4(n)\}}{E\{s_R^4(n)\} + E\{s_I^4(n)\}}$, with $\theta(k) = \pi/2$ or $\theta(k) = 3\pi/2$ which corresponds to $[h_{1,R}(k), h_{1,I}(k)] = [0, \pm\sqrt{\frac{\rho E\{s_R^4(n)\} + \frac{1}{\rho}E\{s_I^4(n)\}}{E\{s_R^4(n)\} + E\{s_I^4(n)\}}}]$, the following can be verified:

$$D[h_{i,R}(k),h_{i,I}(k)]=$$
$$12\left(E\{s_R^2(n)\}E\{s_I^2(n)\}\frac{\rho E\{s_R^4(n)\}+1/\rho E\{s_I^4(n)\}}{E\{s_R^4(n)\}+E\{s_I^4(n)\}}-E\{s_R^4(n)\}-E\{s_I^4(n)\}\right)$$
$$\times\left(\rho E\{s_R^4(n)\}+1/\rho E\{s_I^4(n)\}\right)<0$$

$$\left[\frac{\partial^2 J_{MMA}}{\partial h_{i,R}^2(k)}\right]_{[h_{i,R}(k),h_{i,I}(k)]=\left[0,\pm\sqrt{\frac{\rho E\{s_R^4(n)\}+1/\rho E\{s_I^4(n)\}}{E\{s_R^4(n)\}+E\{s_I^4(n)\}}}\right]}$$
$$=6E\{s_R^2(n)\}E\{s_I^2(n)\}\frac{\rho E\{s_R^4(n)\}+1/\rho E\{s_I^4(n)\}}{E\{s_R^4(n)\}+E\{s_I^4(n)\}}$$
$$-E\{s_R^4(n)\}-E\{s_I^4(n)\}<0 \qquad (10)$$

Substituting the values listed in Table I into (10) yields,

$|h_{i,R}(k),h_{i,I}(k)|=[0,\pm\sqrt{\frac{\rho E\{s_R^4(n)\}+1/\rho E\{s_I^4(n)\}}{E\{s_R^4(n)\}+E\{s_I^4(n)\}}}]$ as the only two saddle points. Figures 2 and 3 are plotted for two different 32-QAMs (8×4 and 16×2), using (3) to confirm the analysis of the non-square rectangular constellations.

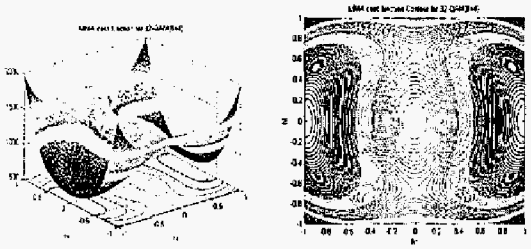

Fig. 2 The 3-D Presentation and Contours for Rectangular MMA

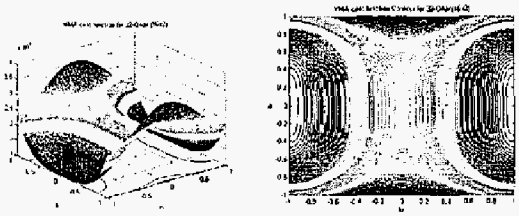

Fig. 3 The 3-D Presentation and Contours for Rectangular MMA

Table I Statistics of rectangular constellations

	$E\{s_R^4\}$	$E\{s_I^4\}$	$E\{s_R^2\}$	$E\{s_I^2\}$	ρ
4x2QAM	41	1	5	1	0.2
8x2QAM	777	1	21	1	0.0476
8x4QAM	777	41	21	5	0.2381
16x2QAM	12937	1	85	1	0.0118
16x4QAM	12937	41	85	5	0.0588
32x2QAM	209033	1	341	1	0.0029

4. Computer Simulations

Computer simulation results are provided to compare the performance of the MMA between using non-square rectangular constellations and using cross constellations. As illustrated in Fig. 1 of [2], the transmitted data symbols $s(n)$ is an independent, identically distributed 32-QAM sequence, and the input to the equalizer $u(n)$ is the sum of the channel output and an independent white Gaussian noise $w(n)$. The real and imaginary parts of the complex-valued additive white Gaussian noise $w(n)$ are assumed to be independent and have equal variance such that the signal noise ratio (SNR) is 30 dB. Simulation experiments described herein employ a complex equalizer of transversal filter structure having 11 tap weights with 5 units of time delay. All the tap weights were initialized by setting the central tap weight to 1 and the others to zero. The step-size parameter, $\mu=10^{-6}$, was used. The complex channel used in the simulations closely follows that from [6]. Figure 4 indicates that the MMA using the non-square rectangular $(8\times4)-QAM$ constellation investigated herein outperforms the MMA proposed by Yang, Werner, and Dumont in [4] for 32-QAM cross constellation. Figure 4(a) was generated by ensemble averaging the squared error $|s(n)-y(n)|^2$ (MSE) versus the number of iterations n over 200 independent learning curves. The resulting equalizer output constellation demonstrates that the MMA proposed in [4] is a rotated version of the constellation used at the transmitter while the MMA using the rectangular constellations is able to recover the phase rotation introduced by channels as depicted in Figs. 4(b) and 4(c).

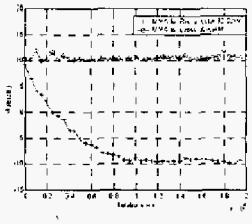

Fig. 4(a) Mean-Squared-Error (MSE) in dB with two different sources

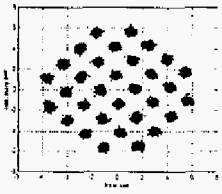

Fig. 4(b) Equalizer output using cross 32-QAM

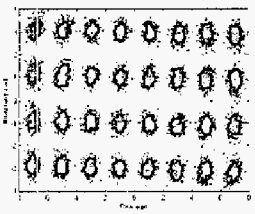

Fig. 4(c) Equalizer output using rectangular 32-QAM

5. Conclusions

N-point QAM constellations ($N = 2^{2i+1}, i \in$ *Integer and* $i \geq 0$) can be divided into two types. One includes cross constellations and the other includes non-square rectangular constellations. The main advantage of adopting the non-square rectangular constellation is that it is better able to recover the phase rotation introduced by channels than can cross and square constellations, because the former has only two local (hence global) minima at $[\pm 1, 0]$, rather than the four global minima in the latter two cases; accordingly, any phase error within 180° can be correctly detected. The two global minima obtained using both cross and square constellations when $\theta(k) \in \left\{\frac{\pi}{2}, \frac{3\pi}{2}\right\}$ correspond to the only two saddle points at $[0, \pm\sqrt{\frac{\rho E\{s_R^4(n)\} + \frac{1}{\rho} E\{s_I^4(n)\}}{E\{s_R^4(n)\} + E\{s_I^4(n)\}}}]$ when the non-square rectangular constellation is used. Another advantage of using the non-square rectangular constellation is that all the four saddle points that are associated with the MMA using both the square and the cross constellations when $\theta(k) \in \left\{\frac{\pi}{4}, \frac{3\pi}{4}, \frac{5\pi}{4}, \frac{7\pi}{4}\right\}$ disappear. Consequently, the MMA using the non-square rectangular constellation may converge more quickly than one that uses other constellations. However, using the non-square rectangular constellation also has disadvantages. First, the non-square rectangular constellation is wider than its square and cross counterparts so the variance of $e(n)$ in the updating of the tap-weight vector of the MMA, i.e.,

$$\mathbf{f}(n+1) = \mathbf{f}(n) - \mu \nabla J_{MMA} = \mathbf{f}(n) - \mu \frac{\partial J_{MMA}}{\partial \mathbf{f}^*(n)} = \mathbf{f}(n) - \mu e^*(n)\mathbf{u}(n)$$

is larger than that obtained using either square or cross constellations. This higher variance increases the tap fluctuations and the associated tap adaptation noise, hindering the opening of the eye. Low tap fluctuation noise can only be maintained by reducing the step size μ ($\mu = 10^{-6}$). However, such a reduction slows the convergence of the equalizer. Additionally, both square and cross constellations require less average transmitted power than does the non-square rectangular constellation.

Acknowledgement

This work was supported by the National Science Council (NSC), Taiwan, R.O.C. under contract NSC 92-2213-E-030-009.

References

[1] Kun-Da Tsai and Jenq-Tay Yuan, "A Modified Constant Modulus Algorithm (CMA) for Joint Blind Equalization and Carrier Recovery in Two-Dimensional Digital Communication Systems," *Seventh International Symposium on Signal Processing and its Applications (ISSPA 2003)*, pp. 563-566.

[2] Kun-Da Tsai and Jenq-Tay Yuan, "Analysis of the Multimodulus Blind Equalization Algorithm for Cross QAM Signal Constellations," *Seventh International Conference on Signal Processing (ICSP'04)*.

[3] G. J. Foschini, "Equalization without altering or detecting data," AT&T Technical Journal, vol. 64, pp. 1885-1911, Oct. 1985.

[4] J. Yang, J.-J. Werner, and G. A. Dumont, "The multimodulus blind equalization and its generalized algorithms," IEEE Journal on Selected Areas in Communications, vol. 20, no. 5, pp. 997-1015, June 2002.

[5] J. Stewart, Calculus, Brooks/Cole Publishing Company, 2nd ed, 1991.

[6] D. Hatzinakos, "Blind Equalization Using Stop-and-go Adaptation Rules," Optical Engineering, vol. 31, no. 6, pp. 1181-1188, June 1992.